

THE ARISING OF ELECTRIC DISCHARGE ARCS

France Pavlovčič, Janez Nastran

University of Ljubljana, Faculty of electrical engineering. Ljubljana, Slovenia

Key words: discharging arc, corona, displacement current, excitation energy, gas ionization.

Abstract: From the viewpoint of electric arcs, electric contacts are systematized due to their mechanic and electric operations in this paper. During the contact operation, drawn and discharging arcs or other discharging phenomena can occur depending on load currents. The difference between the drawn arcs and the discharging arcs is also shown. Further on, the phenomenon of the arising of the discharging arcs from corona is discussed by analyzing this phenomenon through the authors' mathematical model. This model calculates an electron average kinetic energy obtained by its movement along its mean free path in the non-homogeneous electric field between two spherical electrodes. The excitation energy of a gas molecule produced by the electron impact is compared with the first ionization energy and with the dissociation energy of the gas molecule, and the carry-on electron kinetic energy is determined. The displacement current is introduced into the model in the case of the alternating electric field, and its active and reactive component are established due to a complex value of the relative permittivity of the gas. The active component of the displacement current is in the phase with the electric field intensity, and causes the excitation energy in the gas molecules. Ranges of highly ionized, partly ionized and non-ionized molecules are founded in the whole volume. At the end some conclusions are made by comparison of a breakdown voltage obtained by the mathematical model with Paschen's voltage and the measuring result of the discharging arc is also introduced.

Nastanek električnih razelektritvenih oblikov

Ključne besede: razelektritveni oblikov, korona, poljski tok, vzbujevalna energija, ionizacija plinov.

Izvilleček: S stališča električnih oblikov so v tem članku električni kontakti sistemizirani glede na njihovo mehansko in električno delovanje. Med delovanjem kontakta lahko nastanejo potegnjeni in razelektritveni oblikovi ali druge oblike razelektritve, kar je v glavnem odvisno od bremenskega toka. Prikazana je tudi razlika med potegnjenimi in razelektritvenimi oblikovi. Nadalje je obravnavan nastanek razelektritvenih oblikov iz korone z analiziranjem tega pojava s pomočjo matematičnega modela avtorjev članka. Model izračunava povprečno kinetično energijo elektrona, ki jo doseže s preletom svoje srednje proste poti v nehomogenem električnem polju med dvema kroglastima elektrodama. Vzbujevalna energija plinske molekule, ki jo povzroča sila trka elektrona, je primerjana s prvo ionizacijsko energijo in z disociacijsko energijo plinske molekule, obenem je izračunana preostala energija elektrona, ki jo prenese na naslednji trk. Za primer izmeničnega električnega polja je v modelu določen poljski tok in ugotovljeni sta njegova delovna in jalova komponenta glede na kompleksno vrednost relativne dielektričnosti plina. Delovna komponenta je v fazi z električno poljsko jakostjo in povzroča vzbujevalno energijo v plinskih molekulah. V prostoru so ugotovljena območja z visoko vsebnostjo ioniziranih molekul, z delno vsebnostjo ioniziranih molekul in območje brez ionizacije. Na koncu so podani nekateri zaključki s pomočjo primerjave prebojne napetosti, dobljene z matematičnim modelom in Paschenovo napetostjo. Podan je tudi rezultat meritve razelektritvenega oblika.

1. Introduction

Dealing with electric arcs as phenomena occurring between electric contacts, we have to classify the electric contacts according to their mechanic and electric operation. Due to the mechanic operation, the electric contacts are axial switching contacts and sliding contacts. The axial switching contacts have contact members that move in perpendicular direction to contact surface when changing their position. But, with the sliding contacts, their members move along the contact surface that means the parallel moving of both contact surfaces. Due to the electric operation, the electric contacts are making, breaking and holding or permanent. The making contacts establish the electric connection between their members and electric discharge mainly occurs due electric charged capacitance in a circuitry and especially due to a bouncing phenomenon of the making contact members when they close. This paper is not going to deal with that kind of discharges. The breaking electric contacts disconnect the electric circuit and when the contact members are separating from each other, a gap opens between them. In the gap between the contact members, drawn and discharging arcs or other discharging phenomena can occur. The holding or the

permanent contacts have contact members that are touching and the connection is not time-dependent. While the axial switching contacts, when holding, are steady, the sliding contacts are either steady or slipping. The drawn arcs can occur also with the sliding contacts, although they are permanent, such as slip rings, because the microscopic gap between the contact members varies due to the roughness, contamination and damages of the surfaces of both contact members /1/. This paper deals with the discharging arcs, which are stable or unstable since the drawn arcs are discussed in other papers /1/, /2/. The difference between the drawn arc and the discharging arc is in the time-dependent electric current flow through the medium between the contact members when separated. The electric current flow is continuous with the drawn arc and decreases with its length. The medium is the ionized vapour of the cathode and the anode materials. But, with the discharging arc, the current between the separating contact members instantly falls towards zero value, a transient voltage appears due to time derivative of the current, which extends to a breakdown voltage value of the neighbouring gas medium – Fig. 1.

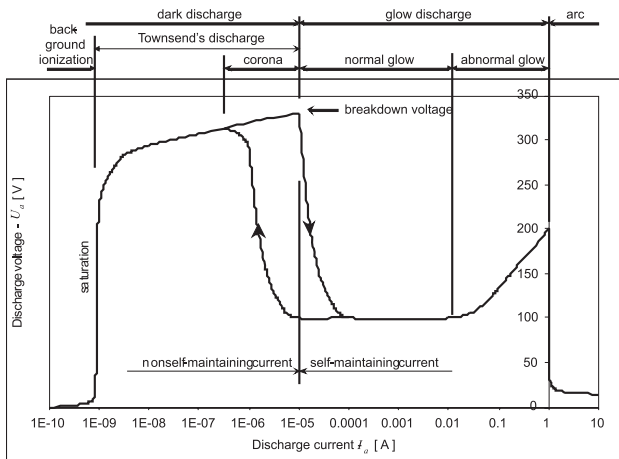


Fig. 1: The principle electric discharge UI characteristics; the discharge current is relative to the infimum arc current.

The medium is an existing gas in the surrounding space. When the breakdown voltage of the gas is exceeded by the transient voltage, the electric breakdown of the insulating gas occurs, the electric current increases. What kind of discharge follows, depends on the current through the gas: the dark discharge, the glow discharge or the discharging arc. The later one is either the stable or the unstable arc. Nevertheless, which arc occurs, it arises from the ionized gas molecules. If there is no existing gas in the surrounding space of the contacts, the discharging arc begins by the ionization of the cathode material vapour. This kind of arcs is vacuum arcs.

Therefore the mathematical model of a spark gap of two spherical electrodes was developed to study the electric field and the ionizing process in the gap. The spherical electrodes were an approximation of the contact members (rivets) with the gap between them when breaking an electric circuit load. The electric load was an inductance-capacitance parallel circuit with a resistance in the inductive branch. The response of the circuit on the breaking manoeuvre was the damped oscillation at the series resonance of the circuit. This circuit represents an air coil in the most simplified way.

2. The mathematical model of a spark gap of two spherical electrodes

The mathematical model is based on two spherical electrodes with the same radius r_0 and separated by the distance d_{sur} between their surfaces. An anode is positively charged and a cathode has a negative charge by the same absolute amount of charge. The cathode is earthed so that there is a positive charge flow from the cathode to the earth. Due to the mutual influence of the anode and the cathode charges, the equivalent point charges of the anode and the cathode lie in the eccentric positions in the relevant spheres – Fig. 2. The mathematical model is solved in two dimensional space because the electric field is rotary sym-

metrical. The eccentric positions of the equivalent point charges are defined by eccentric radius r_{ecc} as it is defined in this paper and shown in Fig. 2, and further on, the eccentric position of the cathode equivalent point charge is the zero point of the coordinate system. A potential of any point $T(r, \varphi) = T(r, r_a)$ in the space is an algebraic sum of the partial potentials caused by the anode and the cathode charges since the potential is scalar value. It is defined by the following equation in the bi-radial coordinates /4/:

$$U(r, r_a) = \frac{Q}{4 \cdot \pi \cdot \epsilon} \left(-\frac{1}{r} + \frac{1}{r_a} \right) \quad (1)$$

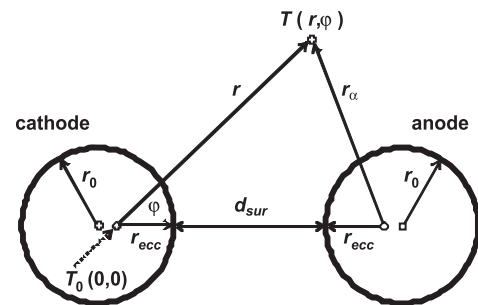


Fig. 2: The geometrical drawing of the cathode, the anode and the distances between them in r - φ coordinate system.

Further on,

$$U(r, \varphi) = \frac{Q}{4 \cdot \pi \cdot \epsilon} \left(-\frac{1}{r} + \frac{1}{\sqrt{(2 \cdot r_{ecc} + d_{sur})^2 + r^2 - 2 \cdot (2 \cdot r_{ecc} + d_{sur}) \cdot r \cdot \cos \varphi}} + \frac{1}{r_{ecc}} - \frac{1}{r_{ecc} + d_{sur}} \right) \quad (2)$$

since the cathode is earthed, its surface potential is defined as zero:

$$r = r_{ecc} \wedge \varphi = 0 \Rightarrow U = 0 \quad (3)$$

Between the anode and the cathode a certain voltage is applied, therefore the anode-cathode voltage is introduced instead of the anode and the cathode charges by using Eq. (2) under the following condition:

$$r = r_{ecc} + d_{sur} \wedge \varphi = 0 \Rightarrow U_{\text{ok}} = \frac{Q}{2 \cdot \pi \cdot \epsilon \cdot r_{ecc} \cdot \left(1 + \frac{r_{ecc}}{d_{sur}} \right)} \quad (4)$$

Hence, the voltage of any point in the space is:

$$U(r, \varphi) = U_{\text{ok}} \cdot \frac{r_{ecc}}{2} \cdot \left(1 + \frac{r_{ecc}}{d_{sur}} \right) \cdot \left(-\frac{1}{r} + \frac{1}{\sqrt{(2 \cdot r_{ecc} + d_{sur})^2 + r^2 - 2 \cdot (2 \cdot r_{ecc} + d_{sur}) \cdot r \cdot \cos \varphi}} + \frac{1}{r_{ecc}} - \frac{1}{r_{ecc} + d_{sur}} \right) \quad (5)$$

The electric field intensity is:

$$\vec{E} = -\text{grad}(U(r, \varphi)) = -\left(\bar{1}_r \cdot \frac{dU(r, \varphi)}{dr} + \bar{1}_\varphi \cdot \frac{dU(r, \varphi)}{r \cdot d\varphi} \right) \quad (6)$$

The radial component of the vector of the electric field intensity is:

$$\vec{E}_r = -\bar{1}_r \cdot \frac{dU(r, \varphi)}{dr} = \bar{1}_r \cdot U_{\text{ax}} \cdot \frac{r_{\text{ecc}}}{2} \cdot \left(1 + \frac{r_{\text{ecc}}}{d_{\text{sur}}} \right) \cdot \left[-\frac{1}{r^2} + \frac{r - (2 \cdot r_{\text{ecc}} + d_{\text{sur}}) \cdot \cos \varphi}{(2 \cdot r_{\text{ecc}} + d_{\text{sur}})^2 + r^2 - 2 \cdot (2 \cdot r_{\text{ecc}} + d_{\text{sur}}) \cdot r \cdot \cos \varphi} \right] \quad (7)$$

and its angular component is:

$$\vec{E}_\varphi = -\bar{1}_\varphi \cdot \frac{dU(r, \varphi)}{dr} = \bar{1}_\varphi \cdot U_{\text{ax}} \cdot \frac{r_{\text{ecc}}}{2} \cdot \left(1 + \frac{r_{\text{ecc}}}{d_{\text{sur}}} \right) \cdot \frac{r \cdot (2 \cdot r_{\text{ecc}} + d_{\text{sur}}) \cdot \sin \varphi}{(2 \cdot r_{\text{ecc}} + d_{\text{sur}})^2 + r^2 - 2 \cdot (2 \cdot r_{\text{ecc}} + d_{\text{sur}}) \cdot r \cdot \cos \varphi} \quad (8)$$

To establish the eccentric radius r_{ecc} as it is defined in Fig. 2, the mathematic inversion on the sphere with the radius of r_0 (known as Kelvin's transformation also) is used and the following result is obtained:

$$r_{\text{ecc}} = \frac{d_{\text{sur}}}{2} \cdot \left(\sqrt{1 + 4 \cdot \frac{r_0}{d_{\text{sur}}} - 1} \right) \quad (9)$$

The shortest field line between the spherical electrodes of the opposite charges is the shortest surface-to-surface distance between the spheres. In this case the angle φ is zero. The vector of electric field intensity has only radial component since the angular component is zero. Hereafter the mathematical model deals with the electric field and the phenomena associated with it in this particular direction. Therefore, the radial coordinate in this direction is named as r_x - radius in the x-direction. Hence the vector of the electric field intensity between the cathode and the anode is:

$$\vec{E} = \vec{E}(r_x) = -\bar{1}_x \cdot E(r_x) \quad (10)$$

where $E(r_x)$ is its absolute value:

$$E(r_x) = U_{\text{ax}} \cdot \frac{r_{\text{ecc}}}{2} \cdot \left(1 + \frac{r_{\text{ecc}}}{d_{\text{sur}}} \right) \cdot \left(\frac{1}{r_x^2} + \frac{1}{(2 \cdot r_{\text{ecc}} + d_{\text{sur}} - r_x)^2} \right) \quad (11)$$

The average velocity of an electron is according to Eq. (8) in literature /1/ as follows:

$$v_{e_avg} = \sqrt{\left(\frac{m_e}{W_{ek}} + \frac{1}{c^2} \right)^{-1}} \quad (12)$$

According to the same equation the average velocity of an air gas molecule (O_2 or N_2) is established by substitution of the electron kinetic energy and mass by the molecule

kinetic energy and mass in Eq. (12), so that the molecule velocity is:

$$v_{m_avg} = \sqrt{\left(\frac{m_m}{W_{mk}} + \frac{1}{c^2} \right)^{-1}} \quad (13)$$

where the kinetic energy of the gas molecule is /6/:

$$W_{mk} = \frac{3}{2} \cdot k \cdot T \quad (14)$$

The mean free path of the electron up to collision with the gas molecule is derived from /5/:

$$\lambda = \frac{R \cdot T}{\sqrt{1 + \frac{v_{m_avg}^2}{v_{e_avg}^2}} \cdot \pi \cdot d^2 \cdot N_A \cdot p} \quad (15)$$

where the quantity d is:

$$d = r_e + r_m \quad (16)$$

The average kinetic energy of the electron travelling along the mean free path is:

$$W_{ek} = e \cdot E(r_x) \cdot \lambda \quad (17)$$

because the electric field intensity and the mean free path are co-linear vectors.

When the electron collided with the gas molecule, its kinetic energy is transferred to the molecule by impact as excitation energy of the molecule:

$$W_{exm} = W_{ek} \quad (18)$$

Following the direction of the cathode-anode gap towards the centre of the gap, these phenomena can occur: the ionization and the recombination of the gas molecules, the dissociation of the gas molecules, and further on, simply no effects on the gas molecules occur by their collision with the electrons. From the gap centre towards the anode these phenomena occur in reverse order. Which phenomenon takes place, and which do not, depends on the kinetic energy of the electrons, which means it depends on the excitation energy of the molecule, as it is defined by Eq. (18).

Due to the decreasing function of the electric field intensity depending on the radius in the range from the cathode to the gap centre, it is established, that there are four possible kinds of collisions with respect to the excitation energy of the molecules along the path between the cathode and the anode as follows:

1. Adjoining the ionization of the gas molecules, the inverse process also takes place. The probability of the ionization is $P_i = 50 \%$ and the probability of the recombination is $(1 - P_i) = 50 \%$. The excitation energy of the molecule is:

$$W_{exm} \geq W_{ion} \quad (19)$$

When this electron collides with the gas particle, there are two possible reactions:

- a. If the gas particle is the molecule, **the ionization** of it takes place. The collision is partly inelastic, and it consumes the ionization energy and the additional electron is emitted from the mole-

cule. After the collision, the average kinetic energy per electron of these two electrons, that is of the one colliding and the one emitted, is:

$$W_{ek_on} = \frac{W_{exm} - W_{ion}}{2} \cdot P_i \quad (20)$$

and it is carried on by each electron to the next collision. After each of them has passed the next mean free path it gets the additional kinetic energy defined by Eq. (17).

- b. If the gas particle is the ion in the neighbourhood of the cathode and the anode, **the recombination** occurs. The collision is totally inelastic, and it consumes the whole kinetic energy of the electron. The excitation energy of the recombined molecule is thermal energy and causes the molecule temperature rise above the ambient temperature for the increment:

$$\Delta T = \frac{2 \cdot W_{exm}}{3 \cdot k} \cdot (1 - P_i) \cdot (1 - K) \quad (21)$$

So far the average temperature of the gas in the neighbourhood of the cathode and the anode rises and the temperature of the each electrode increases too, when the molecules bump at it. The parameter $K=99.8\%$ in Eq. (21) defines the percentage of the excitation energy, conveyed and conducted to the cathode and the anode, and further on, to the ambient as a natural or a forced cooling of both electrodes. Due to the temperature increment of Eq. (21), the average kinetic energy of the gas molecules increases according to Eq. (14), and so the average molecule velocity does according to Eq. (13). The recalculation process is convergent.

2. With the increasing radius, the electric field intensity decreases – Eq. (11), and the excitation energy of the molecule also decreases to such extend that:

$$W_{ion} > W_{exm} \geq W_{diss} \quad (22)$$

In this case, the excitation energy of the gas molecule causes **the dissociation** of the two-atom molecule into two gas atoms. This collision is partly inelastic and it consumes the dissociation energy. The remaining kinetic energy of the colliding electron is carried on by the same electron:

$$W_{ek_on} = W_{exm} - W_{diss} \quad (23)$$

and further on, it increases because the electron passes the next mean free path before the next collision – Eq. (17).

3. If the excitation energy of the molecule is lower than the dissociation energy of the gas molecule:

$$W_{diss} > W_{exm} \quad (24)$$

the colliding electron has **no effect** on the gas molecule. The kinetic energy of the electron is carried on to the next collision because the collision is elastic:

$$W_{ek_on} = W_{ek} \quad (25)$$

The ionization-recombination collisions take place near the cathode, **the dissociation collisions** are next to them

in the direction of increasing radius towards the gap centre and further on, there are **the no-effect collisions**, and follows in the reverse order towards the anode.

Although there is a sequence of these phenomena, we could not consider there are any pure ranges such as an ionization-recombination range, a dissociation range and a no-effect range. But very near to the each electrode there is **a highly ionized range** because the electrons in this range have very high kinetic energy and nearly every collision causes such excitation energy in the molecule that its ionization occurs. Next to this range is **a partly ionized range** up to the point where no ionization occurs. At this point **a non-ionized range** begins and lies around the gap centre – Fig. 3.

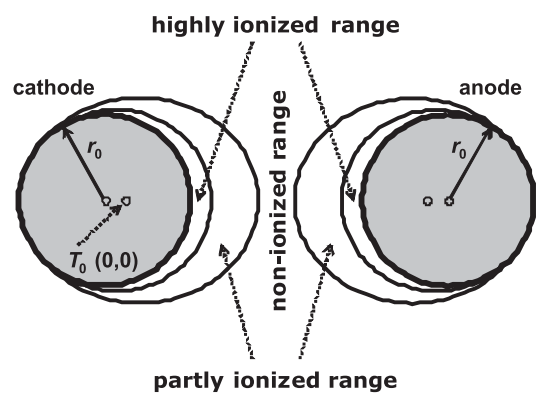


Fig. 3: The ranges of the arising discharge due to switch off manoeuvre in the electric circuit in Fig. 4 at the input-output quantities in Tab. 1 for oxygen molecules as simulated by the model.

In the highly ionized range, the ionization-recombination collisions take place mainly. In the partly ionized range, both the ionization-recombination and the dissociation collisions occur. Further on, in the non-ionized range, there are no ionization collisions, but the dissociation collisions and the no-effect collisions take action. This is the most general situation in the cathode-anode gap and in this case there is no electric breakdown through the cathode-anode gap. If the non-ionized range is not present in this gap along the shortest field line due to the high values of the electric field intensity (caused by the high anode-cathode voltage) and at least the partly ionized ranges come together from the cathode and the anode side, the electric breakdown occurs and electric discharge takes action through a stable or unstable arc, or as a glow discharge with a self-maintaining current.

There were some simplifications made during this modelling process:

1. When deriving Eqs (12) and (13), the following relations were presumed:

$$\begin{aligned} 0 < \frac{v_{e_avg}}{c} &\ll 1 \\ 0 < \frac{v_{m_avg}}{c} &\ll 1 \end{aligned} \quad (26)$$

- The rest and the actual masses of the electron and the gas molecule correspond to:

$$\begin{aligned} m_e &\ll m_m \\ m_e(v_e) &\ll m_m(v_m) \end{aligned} \quad (27)$$

- The ionizations and the recombinations take place in the same range that is in the highly ionized and in the partly ionized range, which lies by the both electrodes.

Knowing the electric field intensity at the cathode surface at $\varphi = 0$ and its temperature, the following conductive current densities are calculated: the current density of the field emission and the current density of the thermionic emission. Both of them are the active current densities.

The current density of the field emission is calculated by the Fowler - Nordheim equation /1/:

$$j_E = \frac{e^2}{8 \cdot \pi \cdot h \cdot \frac{m_e^*}{m_e}} \cdot \frac{E^{*2}}{V_{\phi K}^*} \cdot e^{-\frac{8 \cdot \pi \cdot \sqrt{2 \cdot m_e^* \cdot e \cdot V_{\phi K}^{*3/2}}}{3 \cdot h} \cdot \frac{E^*}{V_{\phi K}^*} + \frac{\sqrt{8 \cdot m_e^* \cdot e^3}}{3 \cdot h \cdot \epsilon_0} \cdot V_{\phi K}^{* -1/2}} \quad (28)$$

Possible thin insulation of the cathode and the roughness of the cathode surface effect the electric field intensity, the work function and the effective electron mass /1/. Therefore the following substitutions must be considered in Eq. (28) to describe exploitation condition of the cathode:

$$\begin{aligned} E^* &= \beta \cdot E && \Leftarrow && \beta = 5 \\ V_{\phi K}^* &= \frac{V_{\phi K}}{\nu} && \Leftarrow && \nu = 5 \\ m_e^* &= \frac{m_e}{\mu} && \Leftarrow && \mu = 5 \end{aligned} \quad (29)$$

but the values of these coefficients were presumed in the model.

The current density of the thermionic emission is defined according to /5/ as:

$$j_T = \frac{4 \cdot \pi \cdot m_e \cdot e \cdot k^2}{h^3} \cdot T_K^2 \cdot e^{\frac{e}{k \cdot T_K} \left(\frac{V_{\phi K}}{\nu} + \sqrt{\frac{e \cdot \beta \cdot E}{4 \cdot \pi \cdot \epsilon_0}} \right)} \quad (30)$$

The direct electric field was dealt with up to this point. If an alternating electric field is applied, a displacement current occurs, which has the following properties essential to establish the mathematical model of electric discharge:

- The displacement current could be measured inside the gas gap between the cathode and the anode.
- There are no current carriers (electrons and ions) in the gap due to this phenomenon.
- There is no rise in electric field intensity due to this phenomenon, so the field emission of the electrons is unchanged.
- This current causes no heat dissipation on the cathode surface, therefore there is no rise in temperature, and further on, there is no rise in the thermionic emission of electrons due to this phenomenon.

- The active component of this current causes the excitation of the two-atom gas molecules and further on the ionization and the dissociation of these molecules.
- The reactive component of this current causes that the electric energy is stored in the capacitance.
- Consequently to the ionization of the gas molecules, the recombination of the gas ions occurs, the thermal energy of the recombined gas molecules increases, but this rise is the effect of the recombination process, and not the effect of the displacement current.

The displacement current is defined in general by its density /4/ as:

$$\hat{j}_D = \tilde{\epsilon}_r \cdot \epsilon_0 \cdot \frac{d\hat{E}(r_x, t)}{dt} \quad (31)$$

The displacement current is complex current density (represented by a phasor) through the capacitance between the cathode and the anode. The relative permittivity $\tilde{\epsilon}_r$ is complex scalar quantity defined by its absolute value e_r and by losses angle d as follows:

$$\tilde{\epsilon}_r = \epsilon_r \cdot e^{-i\delta} \quad (32)$$

Further on, the absolute value of the active displacement current is:

$$j_{Dact} = \epsilon_r \cdot \epsilon_0 \cdot \frac{dE(r_x, t)}{dt} \cdot \sin \delta \quad (33),$$

and it is the one that causes the excitation of the molecules and the phasor of this current density is co-linear with the phasor of the electric field intensity – Fig. 5, so as the phasors of the field and the thermionic emission current densities.

The reactive displacement current is capacitive current and its absolute value is as follows:

$$j_{Dreac} = \epsilon_r \cdot \epsilon_0 \cdot \frac{dE(r_x, t)}{dt} \cdot \cos \delta \quad (34)$$

Therefore the absolute value of the apparent displacement current density is:

$$j_{Dapp} = \epsilon_r \cdot \epsilon_0 \cdot \frac{dE(r_x, t)}{dt} \quad (35)$$

The damping sinusoidal anode-cathode voltage /7/, which is the response of the circuit in Fig. 4 on the switch off manoeuvre, is applied, and hereby the electric field intensity has the same shape and frequency as the anode-cathode voltage:

$$\hat{u}_{\alpha K}(t) = -1 \cdot U_C \cdot e^{-\alpha t} \cdot e^{i(\omega_0 t - \zeta - \xi)} + U_g \quad (36)$$

A phase angle ζ due to $U_C(0)$ and $I_L(0)$ and a phase angle ξ due to α and ω are equal because the inductance and the capacitance in Fig. 4 have no losses, otherwise the angle ζ is smaller then the angle ξ .

The electric field intensity is according to Eq. (11) equal:

$$\begin{aligned} E(r_x, t) &= \text{Re}(\hat{u}_{\alpha K}(t)) \cdot \frac{r_{ecc}}{2} \cdot \left(1 + \frac{r_{ecc}}{d_{sur}} \right) \cdot \\ &\cdot \left(\frac{1}{r_x^2} + \frac{1}{(2 \cdot r_{ecc} + d_{sur} - r_x)^2} \right) \end{aligned} \quad (37)$$

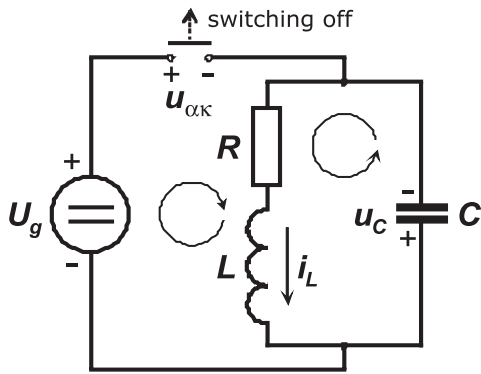


Fig. 4: The electric circuit switched off by the breaking contact.

The time derivative of the anode-cathode voltage is:

$$\frac{d\hat{u}_{\alpha k}(t)}{dt} = U_C \cdot \sqrt{\alpha^2 + \omega_0^2} \cdot e^{-\alpha t} \cdot e^{i(\omega_0 t - \zeta)} \quad (38)$$

Using Eqs (32), (37) and (38) the phasor of the displacement current density is obtained:

$$\hat{j}_D(t) = J_D \cdot e^{-\alpha t} \cdot e^{i(\omega_0 t - \zeta - \delta)} \quad (39)$$

and further on, its apparent value is:

$$j_{Dapp}(r_x, t) = \epsilon_r \cdot \epsilon_0 \cdot \text{Re} \left(\frac{d\hat{u}_{\alpha k}(t)}{dt} \right) \cdot \frac{r_{ecc}}{2} \cdot \left(1 + \frac{r_{ecc}}{d_{sur}} \right) \cdot \left(\frac{1}{r_x^2} + \frac{1}{(2 \cdot r_{ecc} + d_{sur} - r_x)^2} \right) \quad (40)$$

Hereafter the shorter format of the following functions is used:

$$E = E(r_x, t) \quad (41)$$

$$\frac{dE}{dt} = \frac{dE(r_x, t)}{dt}$$

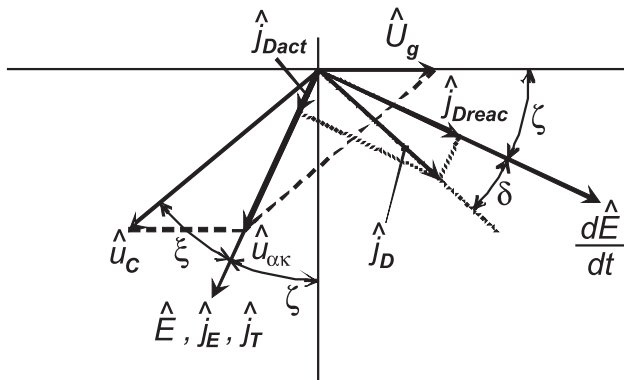


Fig. 5: The principle phasor diagram at $t = 0$ and $\varphi = 0$; not in the scale, because the angles are very small: $\zeta = \xi = 0.0055$ and $\delta = 0.00016$ radians.

Because the active displacement current causes the excitation of the molecule in the volume between the cathode and the anode, the active displacement energy is the integral of the scalar product of the phasors of the active displacement current and the electric field intensity through-

out the volume. Hence, the cosine function of the angle between two phasors is applied, and it is equal to sine function of the complementary angle. So the excitation energy of one molecule in the volume, containing N_m gas molecules, due to the displacement current density is:

$$W_{Dact} = \frac{1}{N_m} \cdot \int_0^t \iiint_{V(N_m)} \hat{j}_D \cdot \hat{E} \cdot dV \cdot dt =$$

$$= \frac{1}{N_m} \cdot \int_0^t \iiint_{V(N_m)} j_{Dapp} \cdot E \cdot \sin \delta \cdot dV \cdot dt = \quad (42)$$

$$= \frac{1}{N_m} \cdot \int_0^t \iiint_{V(N_m)} \epsilon_r \cdot \epsilon_0 \cdot \frac{dE}{dt} \cdot E \cdot \sin \delta \cdot dV \cdot dt$$

Supposing the electric field is homogeneous in the volume V , which contains N_m gas molecules. The displacement energy in this volume is homogeneous also, which means that its density is equal in the gas molecules themselves and in the hollow volume around them. The displacement energy in the gas molecules causes the excitation of the molecules, so this part of the displacement energy is active. The displacement energy in the hollow volume is reactive. To obtain the homogeneous electric field, the smallest volume $V = V(1)$ has to be taken, and this is such one that contains only one gas molecule under the constant thermodynamic conditions of the gas. Hence, this volume must be the greatest one to be equally distributed among all N_m gas molecules. Further on, the active displacement energy of one molecule is defined under the following condition $V_m \ll V(1)$ by:

$$W_{Dact} = \lim_{V(N_m) \rightarrow V(1)} \left(\frac{1}{N_m} \cdot \int_0^t \iiint_{V(N_m)} \epsilon_r \cdot \epsilon_0 \cdot \frac{dE}{dt} \cdot E \cdot \sin \delta \cdot dV \cdot dt \right) =$$

$$= \int_0^t \iiint_{V(1)} \epsilon_r \cdot \epsilon_0 \cdot \frac{dE}{dt} \cdot E \cdot \sin \delta \cdot dV \cdot dt \approx \quad (43)$$

$$\approx \int_0^t \iiint_{V_m} \epsilon_r \cdot \epsilon_0 \cdot \frac{dE}{dt} \cdot E \cdot dV \cdot dt \approx \int_0^t j_{Dapp} \cdot E \cdot V_m \cdot dt$$

Taking into account Eqs (17), (20), (23) and (25), the electron kinetic energy just before the collision with the gas molecule is:

$$W_{ek} = e \cdot E \cdot \lambda + W_{ek-on} \quad (44)$$

This equation forms the calculation loop with Eq. (12), but the mathematical process converges, and the result uniformly exists.

The mathematical model of the electric discharge in gases has to take into account both, the kinetic energy of the electrons and the energy of the displacement current. The electron kinetic energy is partly transferred to the gas molecule by the electron impact, and causes the ionization or the dissociation, discussed heretofore. In this case, the ionization is considered as the impact ionization although it is more probable that the ionization is done through the excitation of the gas molecule on its higher energy level /5/. The dissociation of the two-atom molecule just cannot be carried out directly by the electron impact due to

the large difference of the electron mass and the dissociated atom mass – Eq. (27). The dissociation is completed by the excitation energy of the two-atoms molecule due to the impact energy when raised in such extend that the dissociation energy level is achieved. This is the dissociation due to the conductive current. The displacement current energy also affects the gas molecules, and also causes their ionization and their dissociation. Because it has no carriers, the ionization and the dissociation are caused by the excitation of the gas molecule with no impact, but only due to the displacement current. All these processes: the impact ionization, the dissociation due to the conductive current, the ionization and the dissociation due to the displacement current have the same mechanism of being completed – the excitation of the molecule on its higher energy level, and afterwards the accomplishment of the process. Therefore the kinetic energy Eq. (44) and the displacement energy Eq. (43) are summarized in the excitation energy of the gas molecule, which is the active energy:

$$\begin{aligned}
 W_{exm}(r_x, t, T, W_{ion}, W_{diss}) &= e \cdot E(r_x, t) \cdot \lambda(T) + \\
 &+ W_{ek_on}(W_{ion}, W_{diss}) + \\
 &+ \int_0^t \epsilon_r \cdot \epsilon_0 \cdot \frac{dE(r_x, t)}{dt} \cdot E(r_x, t) \cdot V_m \cdot dt
 \end{aligned}
 \tag{45}$$

This equation is in the calculation loop with Eq. (18) but the calculation converges.

The excitation energy is calculated by Eq. (45), and the minimal value of the excitation energy is graphically represented by the diagram in Fig. 6. The minimal value of the excitation energy is the one without the carry-on kinetic energy of the colliding electron. The gas used in this calculation is oxygen. The highly ionized range begins closely to the electrode and ends where the minimal value of the excitation energy decrease under the value of the ionization energy. The number of the ionized molecules is constant due to the radius and its level is hundred percent of molecules. This range comes out as corona. Closely to it, the partly ionized range begins where the minimal value of the excitation energy is lower than the ionization energy and higher than the dissociation energy, but the carried-on kinetic energy raises the excitation energy on a higher energy level than the ionization energy. It ends where the minimal value of the excitation energy decreases under the dissociation energy because the carried-on kinetic energy is not sufficient to raise the excitation energy on the ionization energy level. The number of the ionized molecules decreases to zero. The number of dissociated two-atom molecules increases up to hundred percent level. In the non-ionized range, where the minimal value of the excitation energy is under the value of the dissociation energy and the carried-on kinetic energy raises the excitation energy up to the dissociation energy level. The number of the dissociated molecules decreases, but the number of the unaffected molecules increases with the radius near centre of the cathode-anode gap.

If the anode-cathode voltage increases, the non-ionized range in Fig. 3 narrows, and the partly ionized range from the cathode side touches the partly ionized range from the anode side, and the ionized path between the electrodes arises, the electric breakdown occurs and the electric discharge arc takes place. Consequently the definition range of the percentage of unaffected molecules, which is on the abscise of the diagram in Fig. 6, limits to zero, and the percentage of the ionized molecules is above zero throughout the whole abscise range. This change in the mathematic functions of the percentage of the ionized and of the unaffected molecules means the establishment of the ionized path between the electrodes.

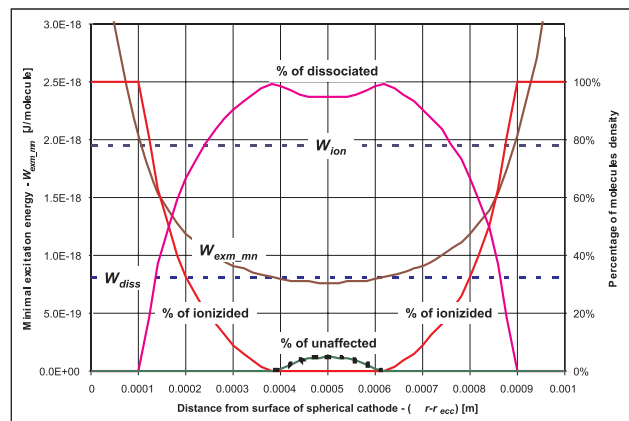


Fig. 6: The minimal excitation energy of the oxygen molecule versus the distance from surface of the cathode to any point at $\varphi = 0$ towards the anode, and the percentage of the oxygen molecules density at the input-output quantities in Tab. 1.

The simulation was carried out with the spherical cathode and anode with the radii of 0.5 mm, and with the surface-to-surface distance of 1 mm between them. The excitation energy in comparison with the first ionization, and with the dissociation energy of the oxygen molecule, and further on, the density of the ionized, the dissociated and the unaffected oxygen molecules are shown in Fig. 6. The input and output quantities of the spark gap discharge model are numerically stated in Tab. 1.

When discussing the electrical breaking contact, its contact members are the electrodes. The distance between them increases from zero, when the breaking contact still holds the closed position, up to the maximum value. In the model, the distance of 1 mm is used because the Paschen law minimum is being avoided. The Paschen law is described by the family of functions of the breakdown voltage of the spark gap depending on the product of the gap length and the gas pressure, but the functions differ by the chemical composition of the gas medium in the gap. These functions have minima: 450 V at 9.2 μm with oxygen, 251 V at 8.8 μm with nitrogen, and 327 at 7.5 μm with air at the same pressure 101.325 kPa in all three cases /8/. At the distances lower than the ones of the minima, the break-

Tab. 1: The input-output table of the spark gap discharge model of oxygen and nitrogen molecules at the same environmental conditions; the variables of the functions are (r, ϕ, t).

medium	O ₂	N ₂	
cathode	Ag	Ag	
W_{ion}	1.955	2.464	aJ/particle
W_{diss}	0.816	1.266	aJ/particle
r_0	0.500	←	[mm]
d_{sur}	1.000	←	[mm]
T_{amb}	293.15	←	[K]
p	101.325	←	[kPa]
U_g	220	←	[V]
R	3.75	←	[kΩ]
L	11.0	←	[H]
C	94.0	←	[pF]
t_0	17.0	←	[μs]
$U_{ox}(t_0)$	10.126	←	[kV]
$j_{Dact}(r_{ecc}, 0, t_0)$	1.49	1.21	[mA/m ²]
$j_{Dreac}(r_{ecc}, 0, t_0)$	9.55	←	[A/m ²]
$(j_E + j_T)(r_{ecc}, 0, t_0)$	6.78	←	[A/m ²]
$dE/dt(r_{ecc}, 0, t_0)$	1.08	←	[TV/m/s]
$E(r_{ecc}, 0, t_0)$	20.3	←	[MV/m]
$E(r_{ecc} + d_{sur}/2, 0, t_0)$	6.75	←	[MV/m]
T	467	531	[K]
d_{diss_B}	0.11	0.07	[mm]
d_{ion_E}	0.39	0.17	[mm]
non-ionized gap	0.22	0.66	[mm]
voltage of non-ionized gap	1.51	5.16	[kV]
ionized	38%	21%	
dissociated	61%	63%	
unaffected	1%	16%	

down voltages are higher than minimal voltages, and with the distances above, the breakdown voltage increases nearly linearly; greater the distance is, more linear the function of the breakdown voltage is. Hence the cathode-anode distance of 1 mm is used in modelling the spark gap phenomena. The Paschen law is also explained by this model: there is a cathode-anode distance at which the majority of the electrons do not achieve enough kinetic energy by moving along the electric field lines to ionize the gas molecules by their impact; and when this cathode-anode distance shortens, it is comparable with the mean free path of the electron, and therefore there is a very small

number of impacts; further on the electric field intensity has to be increased, and hence the anode-cathode voltage, to obtain such electron kinetic energy to excite the gas molecules up to ionized state. The increased anode-cathode voltage is needed with the cathode-anode distance decreased under the certain value, which defines the minimum of Paschen's voltage function. But, this phenomenon is not incorporated in the model because it is no need to be included with the spherical electrodes. The electric field lines between two opposite charged spherical electrodes arise from the anode and sink at the cathode, virtually as their eccentric points are charged. The length of the electric field lines vary from the value of the electrodes surface-to-surface distance to the infinite value and depends on the angular coordinate ϕ, as it is defined in Fig. 2.

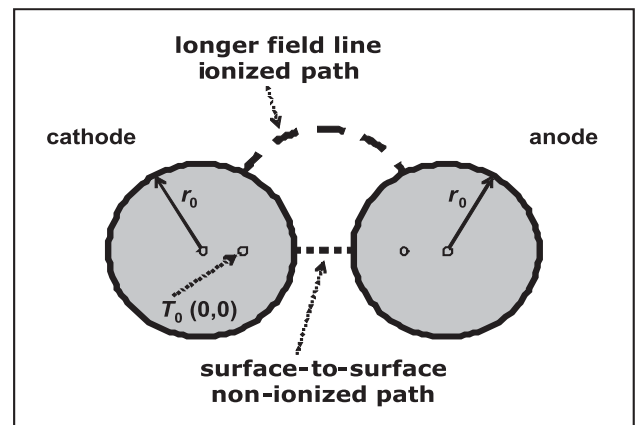


Fig. 7: The formation of the ionized path at the very narrow electrodes surface-to-surface distance.

If the electrodes surface-to-surface distance is too small to establish the electric breakdown, the ionized path is formed along the other longer electric field line – Fig. 7. Hence, dealing with the spherical electrodes, the breakdown voltage and its corresponding path length are always equal or greater than their respective values of the Paschen voltage minimum.

3. The electric arc measurements

The measurement of the discharging arc was carried out, when the air coil, represented by the equivalent electric circuit of the conceptual concentrated electric elements in Fig. 4, was switched off by the breaking contacts of silver. The infimum arc voltage of silver is 12 V and its infimum arc current is 400 mA [9]. The load current was 60 mA, so the drawn arc was unable to be established [1]. The discharging arc began at the instant of 2.4 ms as shown in Figs 8 and 9 when the current dropped towards zero as seen on the oscilogram in Fig. 9.

The time derivative of the current induced the overvoltage, which caused the electric breakdown and the discharging arc was ignited. The arc voltage was 270 V at the beginning and 440 V at the end. Its duration was 2.4 ms.

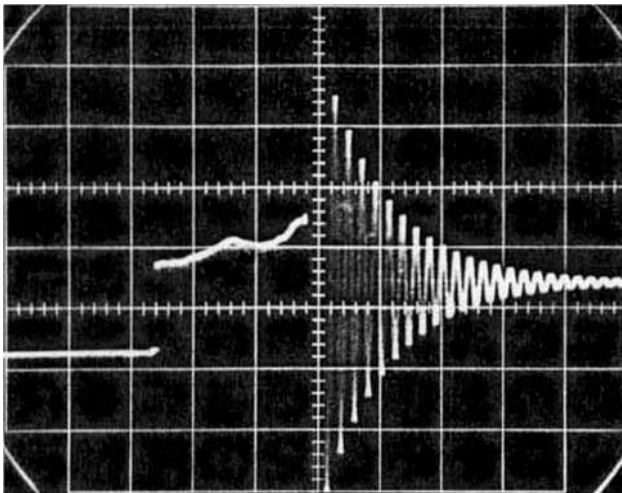


Fig. 8: The discharging arc voltage breaking the inductive load represented by RLC circuit in Fig. 4 and Tab. 1 at the voltage scale 200 V/div. and at time scale 1 ms/div.

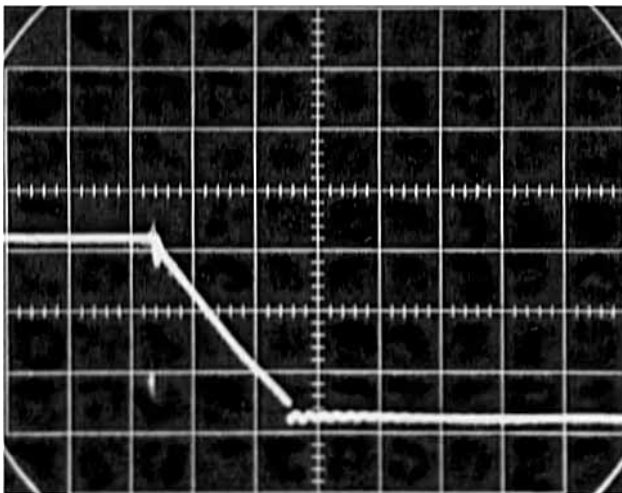


Fig. 9: The discharging arc current breaking the inductive load represented by RLC circuit in Fig. 4 and Tab. 1 at the current scale 20 mA/div. and at time scale 1 ms/div.

To compare the discharging arc with the drawn arc, the latter one was measured too.

The electric contact under the measurement was the commutator sliding contact with the brush of carbon and the commutator bar of copper. In this combination, the carbon infimum arc voltage prevails over the copper one, but the contrary is with the infimum arc current /1/. The infimum arc voltage of carbon is 20 V and its infimum arc current is 30 mA, and 13 V and 430 mA respectively for copper /9/. The drawn arc ignited at the instant of 24 μ s as shown in Fig. 10. The arc voltage was around 20 V throughout the arc duration, and the current was continuous at the instant of ignition. The load was inductive since it was a dc commutator motor. The sliding contact was moving from holding to breaking operation during the arc, which is seen at the end of the drawn arc as a slight overvoltage.

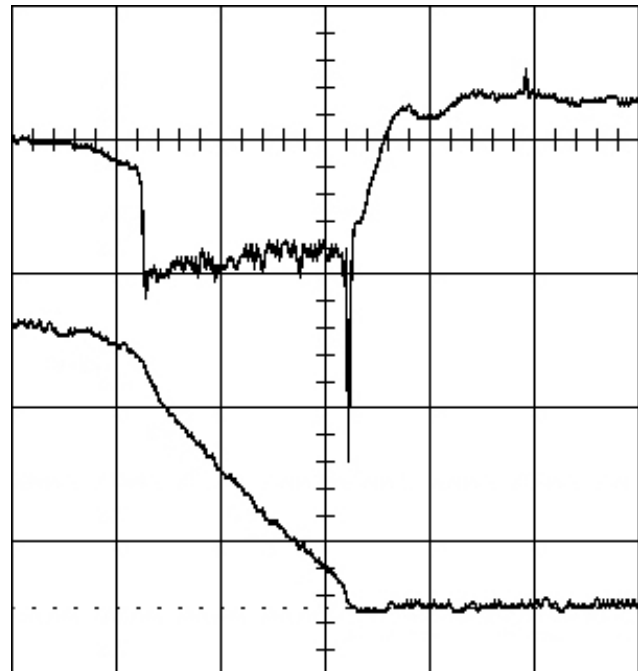


Fig. 10: The drawn arc voltage (upper diagram) and current (lower diagram) of a sliding contact of a commutator with an inductive load at the voltage scale 20 V/div. and the current scale 0.5 A/div. and at time scale 20 μ s/div.

The differences between the discharging and the drawn arcs are clearly seen by the comparison of the oscillograms and the data of both arcs including the contact material properties concerning arcs.

4. Conclusions

Understanding the process of the discharging arc ignition and of the drawn arc also /1/, the arc avoiding and the arc extinguishing methods are established and same old methods are proved to be effective. Some of them are following:

- avoiding the discharging arcs by electric contacts in vacuum because there are no medium to be ionized;
- avoiding the discharging arcs and the drawn arcs also by the wetted electric contacts, which enable wider initial contacts gaps than solid contacts;
- avoiding the discharging and the drawn arcs by capacitance parallel to inductive loads to minimize the displacement current and the peak value of the overvoltage;
- avoiding the discharging and the drawn arcs by capacitance parallel to the electric contacts to bypass the contact current;
- extinguishing the discharging and the drawn arcs by the application of magnetic field perpendicular to the electric field lines in the contact gap to lengthen the path of the electron flow.

There is also the principle of avoiding the drawn arcs, which works effectively just with this kind of arcs, and it is based on the right selection of contact materials /1/, /2/.

5. Used symbols

The symbols used with complex scalars, phasors and vectors of appropriate quantities:

\tilde{a}, \tilde{A}	... complex scalar a, A
\hat{a}, \hat{A}	... phasor a, A
\vec{a}, \vec{A}	... vector a, A
a, A	... absolute value a, A – dc or peak; small letter is instantaneous value

The symbols used with quantities:

\vec{l}_φ	... angular unit vector
\vec{l}_r	... radial unit vector
\vec{l}_x	... radial unit vector at $\varphi = 0$
α	... damping factor of series RLC circuit
β	... enhancement factor of electric field intensity
δ	... losses angle
ε	... permittivity of the dielectric substance
ε_0	... permittivity of vacuum
ε_r	... dielectric constant
ζ	... phase angle due to $U_C(0)$ and $I_L(0)$
ι	... square root of (-1)
λ	... electron mean free path
μ	... factor between rest and effective electron mass
ξ	... phase angle due to α and ω_0
ν	... decreasing factor of work function
φ	... angular coordinate
ω_0	... natural resonant frequency of series RLC circuit
c	... light velocity in vacuum
C	... capacitance
d_{diss_B}	... electrode surface to beginning point of dissociation
d_{ion_E}	... electrode surface to ending point of ionization
d_{sur}	... electrodes surface-to-surface distance
e	... elementary charge
E	... electric field intensity (also instantaneous value)
E_φ	... angular component of electric field intensity
E_r	... radial component of electric field intensity

E^*	... enhanced electric field intensity
e^x	... exponential function
h	... Planck constant
$I_L(0)$... inductance current at $t = 0$
j_D	... displacement current density (instantaneous value)
j_{Dact}	... active displacement current density (instantaneous value)
j_{Dapp}	... apparent displacement current density (instantaneous value)
j_{Dreac}	... reactive displacement current density (instantaneous value)
j_E	... current density due to cold emission (instantaneous value, conductive current)
j_T	... current density due to thermionic emission (instantaneous value, conductive current)
J_D	... displacement current density (peak value)
k	... Boltzmann constant
K	... coefficient of conveyed and conducted thermal energy
L	... inductance
m_e	... rest electron mass
m_e^*	... effective electron mass
m_m	... rest molecule mass
N_A	... Avogadro number
N_m	... number of molecule
p	... gas pressure
P_i	... ionization probability
Q	... electric point charge
r	... radial coordinate
r_α	... radial coordinate from anode eccentric point
r_0	... electrode radius
r_{ecc}	... eccentric electrode radius
r_x	... radial coordinate at $\varphi = 0$
R	... resistance
R	... general gaseous constant in Eq. (15)
$\text{Re}()$... real component of complex scalar or phasor
t	... time
t_0	... time of observation in Tab. 1
T	... gas temperature
T_κ	... cathode temperature
T_{amb}	... ambient temperature
$u_{\alpha\kappa}$... anode-cathode voltage (ac, instantaneous value)
u_C	... capacitance voltage (ac, instantaneous value)
U	... voltage, potential (dc)
$U_{\alpha\kappa}$... anode-cathode voltage (dc or peak value)

U_C	...	capacitance voltage(dc or peak value)	/5/	Sproull, R.L.: <i>Modern Physics</i> , second edition, John Wiley & Sons, Inc., New York - London, 1966.
$U_C(0)$...	capacitance voltage at $t = 0$	/6/	Yavorsky, B.; Detlaf, A.: <i>Handbook of Physics</i> , English translation, Mir publishers, Moscow, 1975.
U_g	...	dc generator voltage	/7/	PAVLOVČIČ, F.: <i>Matematična analiza navitja tu-ljave in njena aplikacija pri raziskovanju iskrenja</i> (Mathematical analysis of a coil winding and its application in spark phenomenon research), Fakulteta za elektrotehniko, Ljubljana 1979.
v_e	...	instant electron velocity	/8/	Naidu, M.S. and Kamaraju, V.: <i>High Voltage Engineering</i> , 2nd ed., McGraw Hill, 1995. ISBN 0-07-462286-2 http://home.earthlink.net/~jimlux/hv/paschen.htm ; 11.06.2007
v_m	...	instant molecule velocity	/9/	Holm, R.: <i>Electric contacts, theory and application</i> , fourth completely rewritten edition, Springer - Verlag, Berlin - Heidelberg - New York, 1979.
v_{e_avg}	...	average electron velocity		
v_{m_avg}	...	average molecule velocity		
V	...	volume		
$V_{\phi\kappa}$...	work function voltage		
$V_{\phi\kappa}^*$...	decreased work function voltage		
V_m	...	molecule volume		
$V(N_m)$...	volume of N_m molecules under the same thermodynamic conditions		
W_{diss}	...	dissociation energy per molecule		
W_{ek}	...	electron kinetic energy		
W_{ek_on}	...	electron carried-on kinetic energy		
W_{exm}	...	molecule excitation energy		
W_{ion}	...	energy of 1 st ionization per molecule		
W_{mk}	...	molecule kinetic energy		

Asst Prof. Dr France Pavlovčič, univ.dipl.ing.
University of Ljubljana, Faculty of electrical engineering, Mechatronics Department, Tržaška 25, SI - 1000 Ljubljana, Slovenia
tel.: +386 (0)1 5181 330,
fax: +386 (0)1 4264 647,
E-mail: france.pavlovcic@siol.com

References

/1/ PAVLOVČIČ, F., NASTRAN, J.: *Affinity of contact materials to form the electric drawn arcs*, Inf. MIDEM, sep. 2005, Year 35, No. 3, pp. 148-157, Ljubljana 2005.

/2/ PAVLOVČIČ, France, NASTRAN, Janez. Avoiding drawn arcs between sliding contacts of commutators. V: MIHALIČ, Franc (ur.). EPE-PEMC 2006: conference proceedings. /Piscataway/ : IEEE, cop. 2006, pp. 1808-1813.

/3/ Gershman S.: Structure of Glow Discharge. http://science-education.ppl.gov/SummerInst/SGershman/Structure_of_Glow_Discharge.pdf; 11.06.2007

/4/ Željeznov M.: *Osnove teorije elektromagnetnega polja* (Fundamentals of Electromagnetic Field Theory) Univerza v Ljubljani, Fakulteta za elektrotehniko, Ljubljana, 1971.

Prof. Dr Janez Nastran, univ.dipl.ing.
University of Ljubljana, Faculty of electrical engineering, Mechatronics Department, Tržaška 25, SI - 1000 Ljubljana, Slovenia
tel.: +386 (0)1 4768 282,
fax: +386 (0)1 4264 647,
E-mail: janez.nastran@fe.uni-lj.si

Prispelo (Arrived): 01.02.2008 Sprejeto (Accepted): 28.03.2008